2022 Basin and Range Earthquake Summit (BRES)

Seismology – Tuesday October 18

Session Conveners: Kris Pankow and James Pechmann
(University of Utah Seismograph Stations)

Invited speakers:

Norman Abrahamson	UC Berkeley	Move to non-ergodic Ground-Motion models for PSHA in Utah
Bill Hammond	University of Nevada, Reno	Unbiased and robust estimation of Walker Lane Fault slip rates using spontaneous block modeling
Jeanne Hardebeck	U.S. Geological Survey	Aftershock Forecasting inthe Basin and Range
Mark Petersen	U.S. Geological Survey	U.S. National Seismic Hazard 50-state Model: Science objectives and products
Fred Pollitz	U.S. Geological Survey	Kinematic slip models of four moderate Intermountain West earthquakes of 2020 and 2021

Poster Session:

Kyren Bogolub	Colorado Geological Survey	The Colorado Geological Survey Seismic Network and Colorado's seismically active regions
Michael Bunds	Utah ValleyUniversity	Coulomb stress change from the March 18, 2020 Magna Mw5.7 earthquake and implications for the Wasatch Fault seismic hazard
Andreas G Cordova	University of Utah Seismograph Stations	$M_{W,CODA}$ for shallow and exotic sources in Utah
Konstantinos Gkogkas	University of Utah	Double beamforming ambient noise tomography of the East Bench Fault using a temporary linear array

Seismology – Tuesday October 18

Session Conveners: Kris Pankow and James Pechmann
(University of Utah Seismograph Stations)

Poster Session Continued:

Bill Hammond	University of Nevada, Reno	Bringing recent Basin and Range earthquakes and the seismic cycle into focus with geodetic networks
Lee Liberty	Boise State University	Seismic profiling across the Eglington and Frenchman Mountain faults, Las Vegas, Nevada
Mairi Litherland	New Mexico Bureau of Geology	Recent developments in seismic monitoring in New Mexico
John Louie	Nevada Seismological Laboratory, University of Nevada, Reno	Exploring basin amplification within the Reno metropolitan area with non-ergodic 3D scenarios
Kristine Pankow	University of Utah Seismograph Stations	Modeling aftershock sequences in the eastern Intermountain West
James C. Pechmann	University of Utah, Dept. of Geology and Geophysics	A logic tree for the subsurface geometry of the Salt Lake City segment of the Wasatch Fault in light of the 2020 Magna, Utah earthquake
Gesa M. Petersen	University of Utah Seismograph Stations	Four decades of seismic swarm activity in the transition zone between Basin-and-Range and Colorado Plateau, Central Utah
Israporn Sethanant	University of Victoria	Structural immaturity and tectonic implications of the 2020 Mw 6.5 Monte Cristo Range Earthquake, Nevada: Evidence from near-field and far-field observations
Daniel Wells	University of Utah	Relocating the Utah Magna aftershock sequence using NonLinLoc source-specific station terms, and waveform similarity
Ivan Wong	Lettis Consultants International, Inc.	The implications of a listric Wasatch Fault for seismic hazard along Utah’s Wasatch Front

Seismology – Tuesday October 18

Session Conveners: Kris Pankow and James Pechmann
(University of Utah Seismograph Stations)

Poster Session Continued:

Zachary M. Young	Nevada Geodetic Laboratory	Interseismic strain accumulation across the central Basin and Range: Implications for southern Nevada seismic hazard
Qicheng Zeng	University of Utah	Investigating the 3D basin structure of Salt Lake Valley using surface waves recorded by the Magna aftershock nodal array

MOVE TO NON-ERGODIC GROUND-MOTION MODELS FOR PSHA IN UTAH

Norman Abrahamson, University of California, Berkeley, abrahamson@berkeley.edu
Chih-Hsuan Sung, University of California, Berkeley, karensung@berkeley.edu

ABSTRACT

With the large increase in the number of recorded ground motions, it has become clear that there are large systematic differences in ground-motion scaling within the western US and even within relatively small regions such as the Wasatch Front, Utah. The results from 3-D simulations also show large effects of the 3-D crustal structure on the ground motion at a specific site from a specific source location that cause significant deviations from the average scaling for the region. These observations have led to the move from ergodic to non-ergodic ground-motion models (GMMs). While ergodic GMMs provide a stable estimate of the average ground-motion scaling for a region, they are poor predictors of the ground motion at a specific site from a specific source, and they overestimate the aleatory variability at a single site. Non-ergodic GMMs mimic the source/site-specific effects seen in 3-D simulations by including allowing the coefficients of the GMM to depend on the source and site location.

Sung et al. (2021) developed a non-ergodic GMM using the observed ground motions from about 1500 recordings from 60 small to moderate earthquakes in Utah. The standard deviation of the non-ergodic GMM is about 25% smaller than the ergodic standard deviation. The median values vary by up to a factor of 2 from the average model depending on the site/source pair. In addition, the 3-D simulations for Utah developed by Moschetti et al. (2017) are used to develop a non-ergodic site term for long-period basin effects from large-magnitude earthquakes on the Wasatch fault. The non-ergodic basin terms lead to a range of a factor of 1.5 increase or decrease relative to average scaling based on basin depth terms.

The application of non-ergodic GMMs in PSHA requires three modifications to the ergodic GMMs: (1) reduce the aleatory standard deviation of the ergodic GMM; (2) estimate the source/site-specific adjustment to the median from the ergodic GMM, and (3) estimate the epistemic uncertainty source/site-specific adjustment term. The hazard is computed using the adjusted median and reduced standard deviation with the epistemic uncertainty in the adjustment included in a logic tree. We show examples of hazard for T=0.2 and T=3 sec computed for the Salt Lake region using ergodic and non-ergodic GMMs from both empirical data and 3-D simulations. The mean hazard decreases for 70% of the sites and increases for 30% of the sites due to the skewed distribution of ground motions.

UNBIASED AND ROBUST ESTIMATION OF WALKER LANE FAULT SLIP RATES USING SPONTANEOUS BLOCK MODELING

William C. Hammond, University of Nevada, Reno, whammond@unr.edu
Corné Kreemer, University of Nevada, Reno, cornelisk@unr.edu
Geoffrey Blewitt, University of Nevada, Reno, gblewitt@unr.edu

ABSTRACT

The Walker Lane (WL) in the western Great Basin is a seismically active plate boundary system that accommodates 20-25% of the relative tectonic motion between the Pacific and North American tectonic plates. Domains within the WL have various proportions of dextral, sinistral, normal, or oblique rakes, and varying rates of block rotation. Actively accumulating strain is accommodated by slip on many faults and folds with hundreds of individual segments having a variety of slip styles. Geodetic GPS networks measure the rate, pattern, and style of this active deformation with a precision approaching 0.1 mm/yr per station, at many stations (over 400 in Nevada, and over 160 in Utah). These networks include the MAGNET GPS network operated by the University of Nevada, Reno, the NSF Network of the Americas, and various others.

Key parameters needed to map the hazard associated with this complex system are the fault slip rates. The geodetic velocity field places strong constraints on the broad-scale budgets across extended zones, and on individual faults within the system. Slip rates can be estimated with geodesy by measuring the relative motion of adjacent crustal blocks and solving for slip rate via a model accounting for rotation and shallow locking. However, owing to the large number of faults and complexity of the system, developing detailed block models on a province scale has proven difficult. Moreover, to build analytically viable models subjective choices need to be made about how discontinuous faults connect and interact to accommodate strain. Since results are sensitive to blocks geometry, this can lead to bias in slip rate estimates.

We address this challenge by using a new framework where large numbers of block models are algorithmically generated from the fault geometry database. Each model has slightly different block configurations, but all honor the input fault data, rules of kinematic consistency, modeling regularization, and the GPS data. The approach, called Spontaneous Blocks, provides several advantages over bespoke models. For example, 1) availability of posterior slip rate distribution that objectively characterize uncertainty attributable to incomplete knowledge of the fault connectivity, 2) insensitivity to outliers, and 3) covariance between adjacent fault slip rate estimates. Deformation not occurring on the faults is explicitly recognized and quantified, providing a means to characterize and quantify off-fault deformation.

AFTERSHOCK FORECASTING IN THE BASIN AND RANGE

Jeanne L. Hardebeck, U.S. Geological Survey, jhardebeck@usgs.gov
Michael Barall, U.S. Geological Survey, mbarall@usgs.gov
Sara K. McBride, U.S. Geological Survey, skmcbride@usgs.gov
Andrew J. Michael, U.S. Geological Survey, ajmichael@usgs.gov
Morgan T. Page, U.S. Geological Survey, mpage@usgs.gov
Gabrielle M. Paris, U.S. Geological Survey and Portland State University, gparis@usgs.gov
Nicholas J. van der Elst, U.S. Geological Survey, nvanderelst@usgs.gov

ABSTRACT

Aftershock forecasts can help a wide range of users - including the public, emergency responders, and lifeline engineers - prepare for, respond to, and recover from earthquake disasters. The USGS delivers public forecasts of the probability and expected number of aftershocks following domestic earthquakes M≥5. We have updated the Reasenberg & Jones (Science, 1989) methodology to improve the uncertainty estimates, the handling of early catalog incompleteness, and the Bayesian parameter adaptation as aftershock sequences progress (Page et al., BSSA 2016). The aftershock forecasts are generated automatically, integrated with other earthquake products on the USGS event webpages, and communicated with a template that provides basic aftershock information as well as detailed numerical forecasts. We are working to operationalize ETAS forecasting (Ogata, JASA 1988), which works better for sequences with large aftershocks, and more accurately estimates the forecast uncertainty. We have developed new generic aftershock parameters based on tectonic regionalization (Page et al., 2016). For much of the Basin and Range we use globally derived parameters for active shallow continental regions, while locally-derived parameters are used in California (Hardebeck et al., SRL 2019) and soon in Utah (Mesimeri & Pankow, AGU 2020). The USGS has released forecasts for numerous Basin and Range earthquakes, including: 2019 M6.4 and M7.1 Ridgecrest, CA; 2020 M5.7 Magna, UT; 2020 M5.2 Bodie, CA; 2020 M6.5 Monte Cristo, NV; 2020 M5.8 Lone Pine, CA; and 2021 M6.0 Antelope Valley, CA. The forecasts were successful in that the observed number of aftershocks of various magnitudes generally fell within the ranges given in the forecasts. A few of the longer forecasts (1 month or 1 year) were less accurate, and these were usually made early in the sequence before a sequence-specific decay rate could be determined. The Lone Pine, Ridgecrest, Monte Cristo, and Bodie aftershock sequences, in particular, decayed faster than the generic model. The late M4 Magna aftershocks are consistent with the generic decay. The Ridgecrest forecast suggests that the Lone Pine earthquake was more likely an independent event than an aftershock. The aftershock forecasts have been used to inform the resumption of operations at the China Lake Naval Air Weapons Station following the Ridgecrest earthquakes, and by the State of Utah to determine the duration of the disaster declaration following the Magna earthquake.

U. S. NATIONAL SEISMIC HAZARD 50-STATE MODEL: SCIENCE OBJECTIVES AND PRODUCTS

Mark D. Petersen, U.S. Geological Survey, mpetersen@usgs.gov

ABSTRACT

The U.S. National Seismic Hazard Model (NSHM) is developed periodically by the USGS to account for new and improved data, models, and methods that have been developed since the previous model release. This probabilistic model is applied in building design criteria, risk assessments, and other public policy documents requiring that the best available and defensible science be considered. This 2023 NSHM will consider seismic hazard in all 50 states taking into account inherent differences in geological setting, tectonic strain rates, and earthquake rupture mechanics while allowing for more uniform methodologies and more consistent representation of epistemic uncertainties. Public workshops during 2020 -2021 allowed for critical discussions on important elements of the NSHMs. The 2023 NSHM will be developed over the next two years and will include updates to both the source and ground motion inputs. For the statistical seismicity elements of the source model, we plan to update and decluster earthquake catalogs based on new algorithms, assess gridded seismicity rates using alternative statistical assessments, possibly evaluate application of time-dependent hazard branches, and calculate hazard. For applying new geologic and geodetic data in the source models, we are developing a database of geologic fault rupture rates and geodetic slip rates that will be used to construct multi-fault rupture models. For improving the ground motion models (GMM), we plan to update the CEUS-WUS boundary, implement several new GMM including new NGA-Subduction models, consider how to better implement GMM uncertainty and variability by evaluating new nonergodic methods, and improve the assessment of ground shaking in basins using basin depth information and simulations. Several important implementation issues will also consider better non-linear ground shaking estimates for the CEUS, assessment of hazard near basin edges, and implementation of uncertainty analysis.

KINEMATIC SLIP MODELS OF FOUR MODERATE INTERMOUNTAIN WEST EARTHQUAKES OF 2020 AND 2021

Fred F. Pollitz, U.S. Geological Survey, Moffett Field, fpollitz@usgs.gov
Charles W. Wicks, U.S. Geological Survey, Moffett Field, cwicks@usgs.gov
Jerry Svarc, U.S. Geological Survey, Menlo Park, jsvarc@usgs.gov
William C. Hammond, Nevada Geodetic Laboratory, Nevada Bureau of Mines and Geology, University of Nevada, Reno, whammond@unr.edu
Thorne Lay, University of California, Santa Cruz, tlay@ucsc.edu
Chengli Liu, Institute of Geophysics and Geomatics, China University of Geosciences, Wuhan, China, liuchengli@cug.edu.cn

ABSTRACT

Four large earthquakes struck the Intermountain West and Basin and Range Province in 2020 and 2021: M5.7 March 18, 2020 Magna, Utah; M6.5 March 31, 2020, Stanley, Idaho; M6.5 May 15, 2020 Monte Cristo Range, Nevada; and M6.0 July 8, 2021 Antelope Valley, California, earthquake. As noted by Wesnousky (2020 SRL), each of the first three occurred in areas of relatively high background seismicity and geodetic strain rate; the same is true for the Antelope Valley earthquake. The events sample different tectonic environments with distinct fault geometries, leading to unique rupture characteristics of each event. We explore kinematic slip models of these earthquakes based on observations of geodetic static offsets and seismic waveforms. The Magna and Antelope Valley earthquakes are both normal faulting events that did not approach Earth's surface (centroid depths ~8-10 km). However, their fault dips differ substantially — 30 deg. and 50 deg., respectively, reflecting likely differing tectonic stress fields. The Monte Cristo Range event involves predominantly left-lateral strike slip on steeply dipping faults and normal slip on a small near-surface shallowly dipping fault. The Stanley event is the deepest of the four, with significant slip concentrated at depth ~8 to 16 km. It involves both strike slip and normal slip, with a gradual transition between the two in the along-strike direction, reflecting a spatially variable tectonic stress field. The Stanley and Antelope Valley events involve unilateral rupture propagation, but the Magna and Monte Cristo Range events have bilateral rupture propagation. Geodetic data (GNSS and InSAR) complement seismic waveform data and play important roles in constraining the fault geometry and spatial distribution of slip.

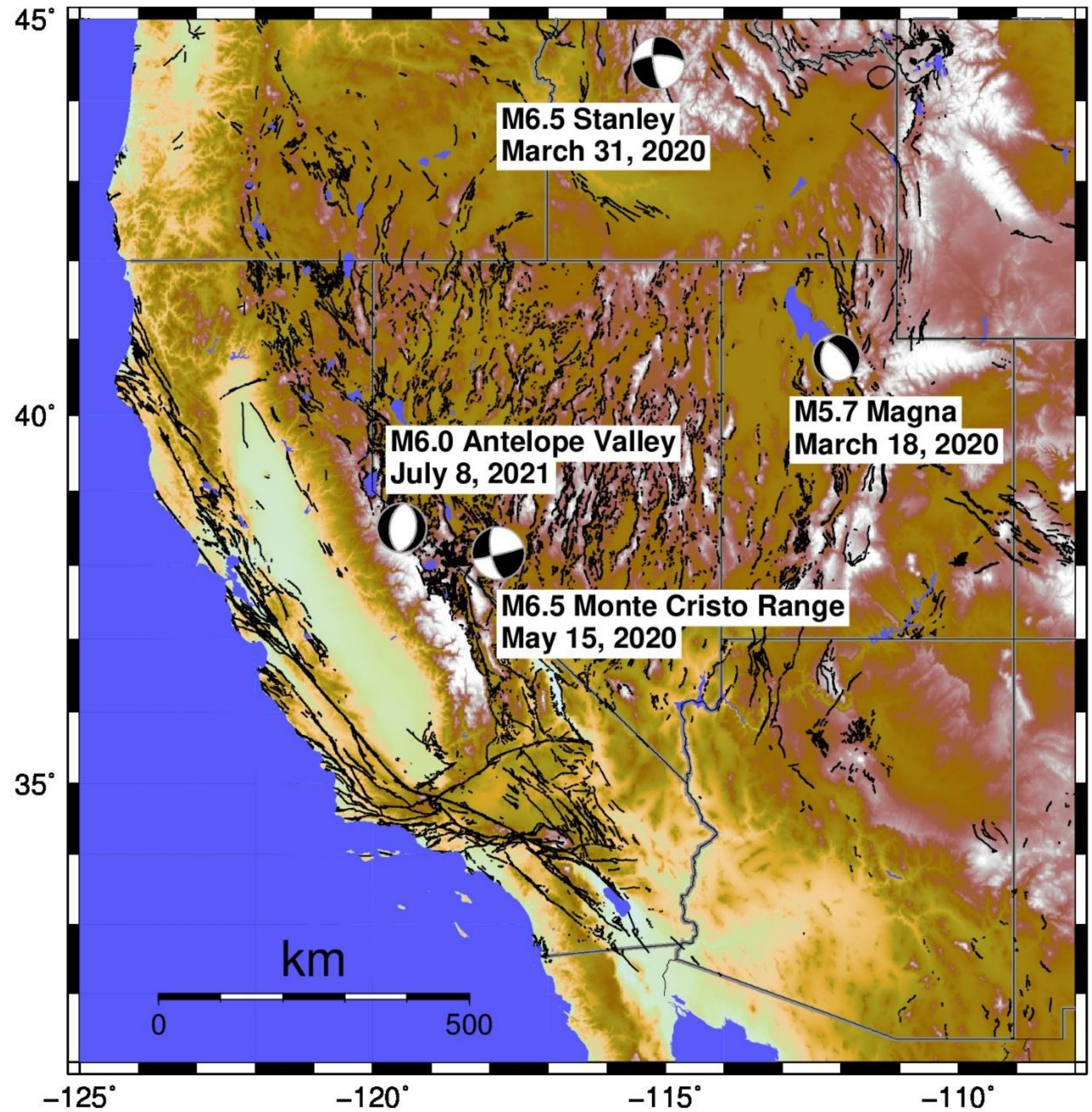

Figure 1. *Locations and focal mechanisms of the notable Intermountain West earthquakes. Superimposed are fault traces from the USGS Quaternary Fault and Fold Database.*

THE COLORADO GEOLOGICAL SURVEY SEISMIC NETWORK AND COLORADO'S SEISMICALLY ACTIVE REGIONS

Kyren Bogolub, Colorado Geological Survey, kbogolub@mines.edu
Matt Morgan, Colorado Geological Survey, mmorgan@mines.edu

ABSTRACT

The Colorado Geological Survey Seismic Network (CGSSN) consists of eight permanent seismic stations. The network is primarily used to locate small magnitude and induced earthquakes throughout the state. We will be presenting on the status of the current network and our goals for the future of the CGSSN in the context of the seismically active regions of the state. This will include a focus on historical earthquakes of Colorado as well as modern earthquake catalogs. We will also highlight some of the lessons we have learned in developing the network and the collaborations that have made the network possible.

COULOMB STRESS CHANGE FROM THE MARCH 18, 2020 MAGNA M_W5.7 EARTHQUAKE AND IMPLICATIONS FOR WASATCH FAULT SEISMIC HAZARD

Michael P. Bunds, Utah Valley University, Michael.Bunds@uvu.edu
Michael A. Stearns, Utah Valley University, MStearns@uvu.edu

ABSTRACT

The March 18, 2020 M_w5.7 Magna earthquake occurred 18 km west of the surface trace of the Salt Lake City (SLC) segment of the west-dipping Wasatch fault (WF) in the populous Salt Lake Valley on the eastern edge of the Basin and Range. The SLC segment is capable of producing a > M7 earthquake and it is late in its seismic cycle (WGUEP, 2016). Published source mechanics and analysis of the distribution of aftershocks show the Magna earthquake was caused by normal-oblique slip on a fault that dips 30 ± 10^o west (UUSS, 2020; Pang et al., 2020). To our knowledge, this is the first recorded moderate to large earthquake on a normal fault that dips ~30^o or less in the Basin and Range. Furthermore, if the WF is listric and dips ~30^o W in the subsurface, then the earthquake likely occurred on the down-dip extension of it (e.g., Pang et al., 2020). To address possible impacts of the Magna earthquake on WF seismic hazard, we calculate Coulomb stress change imparted by slip in the earthquake on receiver faults that model the SLC segment of the WF and estimate changes in future earthquake probability from the stress changes. Our results indicate that if the WF is listric, then Coulomb stress on it has increased significantly no matter if the Magna earthquake occurred on it. In contrast, if the WF dips more than about 45^o in the subsurface and lies to the east of the Magna earthquake source at depth then Coulomb stress and seismic hazard on it probably was reduced. For the scenario that the Magna earthquake occurred on the down-dip extension of the WF, we estimate Coulomb stress increased ~1 b average over ~290 km^2 of area on the SLC segment of the WF. These results are similar to estimated increases prior to large earthquakes apparently triggered by slip on nearby faults (e.g., Hodgkinson et al., 1996; Nalbant et al., 2005; Toda and Stein, 2020). We apply the method of Stein et al. (1997) to estimate the change in future earthquake probability on the WF that could be expected from the Coulomb stress changes. In this method, both transient and long-term effects of Coulomb stress change are incorporated into standard, existing estimates of conditional probability. The transient effect uses rate-and-state friction theory (Dieterich, 1994) to estimate a transient increase in earthquake frequency based on the Coulomb stress change and observed activity increases following other earthquakes. To include the long-term effect, the Coulomb stress change is equated to a length of time to accumulate the same stress change by tectonic loading and then shortening the mean recurrence time accordingly. Our results suggest the Magna earthquake may have increased the 10-year conditional probability of a surface-rupturing earthquake on the WF by a factor of 1.5 to 3.3 (i.e., from ~1.5% to ~2.1 – 5%), and the 50-year conditional probability by factor of 1.1 to 1.5 (i.e., from ~7.5% to ~8.5 – 12%) relative to existing conditional probability estimates (WGUEP, 2016).

$M_{W,CODA}$ FOR SHALLOW AND EXOTIC SOURCES IN UTAH

Andreas G. Cordova, University of Utah, andreascordova98@yahoo.com
Katherine M. Whidden, University of Utah, katherine.whidden@utah.edu
Kristine L. Pankow, University of Utah, pankow@seis.utah.edu
Kevin Mayeda, Air Force Technical Applications Center, kevin.mayeda@gmail.com
William R. Walter, Lawrence Livermore National Lab, walter5@llnl.gov
Rengin Gök, Lawrence Livermore National Lab, gok1@llnl.gov
David Shelly, US Geological Survey, dshelly@usgs.gov

ABSTRACT

Measuring M_w for small earthquakes is desirable in order to have a uniform magnitude catalog to compute accurate catalog statistics, such as b-value, and for earthquake hazard analysis. However, M_w is difficult or impossible to compute for events with M < 3.5 using traditional regional moment tensor analysis. An alternative is the S-wave coda M_w method outlined in Mayeda et al. (2003). $M_{w,coda}$ measurements are very stable due to the coda waves' relative insensitivity to source radiation pattern and path heterogeneity. The $M_{w,coda}$ method has been used to measure M_w in diverse regions worldwide, including the entire state of Utah as well as a more focused study of the March 2020 M_w 5.7 Magna, UT earthquake and its aftershocks (Holt et al., 2021). $M_{w,coda}$ is effective for small magnitude earthquakes, down to approximately Mw,coda 1.5 in Utah. The University of Utah Seismograph Stations (UUSS) has a goal of routinely reporting $M_{w,coda}$ for Utah earthquakes down to at least M_w 2.0.

One complication of the $M_{w,coda}$ method is that shallow earthquakes (depth < ~6 km) have a peak in the low frequency spectra, likely due to Rg-to-S scattering. If the peak is not accounted for, an artificially high $M_{w,coda}$ measurement can result. $M_{w,coda}$ studies in Utah to date have avoided the shallow depth spectral peak problem by excluding shallow events.

Here, we apply the $M_{w,coda}$ method to 40 shallow seismic events in Utah for which we also have waveform-modeled M_w. Seismicity ranges from 1998-2020 in time and $3.25 \leq M_w \leq 4.59$ in magnitude. Many of the events are earthquakes, but some are more exotic sources such as mine collapses and a suspected magmatic intrusion. As expected, we find that the $M_{w,coda}$ method overestimates the size of these shallow events. We observe a distinct split between normal depth (below sea level) and shallow (above sea level) events in a comparison of $M_{w,coda}$ to M_L for all earthquakes from 2021 in the Utah region greater than M 2. Therefore, we calculate a separate $M_{w,coda}$ calibration for shallow events. We explore ways to identify shallow earthquakes when the network is too sparse for reliable catalog depths, including spectral shape and comparison of different magnitude types. With separate calibrations for shallow and deep events, we should be able to incorporate $M_{w,coda}$ into UUSS routine earthquake processing for all earthquakes with M_w > 2.0.

REFERENCES

Holt et al., 2021, SRL, 10.1785/0220200320
Mayeda et al., 2003, BSSA, 10.1785/0120020020

DOUBLE BEAMFORMING AMBIENT NOISE TOMOGRAPHY OF THE EAST BENCH FAULT USING A TEMPORARY LINEAR ARRAY

K.Gkogkas, University of Utah, kos.gkogkas@utah.edu
F.-C. Lin, University of Utah, FanChi.Lin@utah.edu
A.A. Allam, University of Utah, amir.allam@utah.edu

ABSTRACT

We provide new constraints on the shallow structure of the East Bench segment of the Wasatch Fault System by exploiting continuous data recorded from a month-long temporary linear array of 32 nodal stations deployed along 1700 South in Salt Lake City. We cross-correlate the ambient noise records and extract Rayleigh wave signals in the period range 0.4 s to 1.1 s. We apply double beamforming, enhance the signal, measure period-dependent Rayleigh wave phase velocities and construct a 2-D profile. We invert the 1-D phase velocity dispersion curve at each beam center by adapting an uncertainty-weighted least-squares inversion scheme and combine all inverted 1-D Vs models to obtain a pseudo-2D Vs model for the area, mostly sensitive at the upper 400 m beneath the array. The resulting Vs model exhibits faster velocities to the east and slower velocities to the west, in good agreement with the expected thickening of sedimentary deposits towards the center of the basin. Moreover, a 400 m-wide low-velocity zone narrowing with depth is observed proximate to the surface trace of the East Bench fault, suggesting the presence of a fault damage zone. The proposed geometry of the damage zone is asymmetric, being wider on the hanging wall and with greater velocity reduction. Our results provide important information regarding the shallow structure and mechanics of the Wasatch Fault System and for the seismic hazard assessment in Salt Lake City. Furthermore, the good correlation between our model features and the local geologic and tectonic structures encourages more extensive future applications of ambient noise imaging in Salt Lake City.

BRINGING RECENT BASIN AND RANGE EARTHQUAKES AND THE SEISMIC CYCLE INTO FOCUS WITH GEODETIC NETWORKS

William C. Hammond, University of Nevada, Reno, whammond@unr.edu

ABSTRACT

The past two and a half years has seen a cluster of notable earthquakes that have highlighted the seismic hazard driven by active tectonics of the Basin and Range Province. These events not only remind us of the hazard but also supply crucial data that illuminate the connections between the various seismic, geologic, hydrologic and geodetic datasets that pertain to the physical processes at play before, during, and after the events.

In this presentation I will focus on the lessons learned from the May 15, 2020, M 6.5 Monte Cristo Range earthquake (MCR), but also touch on other recent events such as the March 31, 2020, M6.5 Stanley, Idaho earthquake, and the July 8, 2021, M6.0 Antelope Valley earthquake. While these events were widely separated from one another they share a role in the accommodation of active plate boundary tectonic deformation of the Intermountain Western United States. The presentation will highlight their locations within the active background tectonic strain rate field measured by GPS stations from multiple networks currently in operation and past GPS campaigns. The geodetic data are particularly useful for directly assessing the relationship between various aspects of the earthquake cycle, such as interseismic strain accumulation, coseismic strain release, and postseismic deformation. One example is that for each of these events the coseismic strain was in a style consistent with the interseismic tensor strain rate style.

The MCR event is a particularly good example of observations made through multiple stages of the seismic cycle. Following the event data were collected in the dense semi-continuous MAGNET GPS Network in a rapidly mobilized field deployment, supplementing prior data obtained in regular surveying for over 16 years. These data were integrated with those from other GPS networks in the western Great Basin and InSAR data from the ESA Sentinel satellite mission. They were used to create slip models of the event which showed the consistency between pre-event strain accumulation, long-term slip rate on the Candelaria Fault, and post-event after-slip which proceed for at least several months following the origin time.

Thus these data provide a wholistic view of the earthquake cycle in space and time and allow us to make comparisons between various other datasets that pertain to the event such as surface rupture, aftershock seismicity, and impacts on nearby geothermal well chemistry and physical parameters. We can also compare the coseismic parameters inferred from several of the various techniques to identify which are most sensitive to total moment, and what they imply for the tectonic regime of the east-central Walker Lane and Mina Deflection. The presentation will also discuss similar insights gained from the Antelope Valley and Stanley Idaho events via coverage by regional GPS networks and InSAR data.

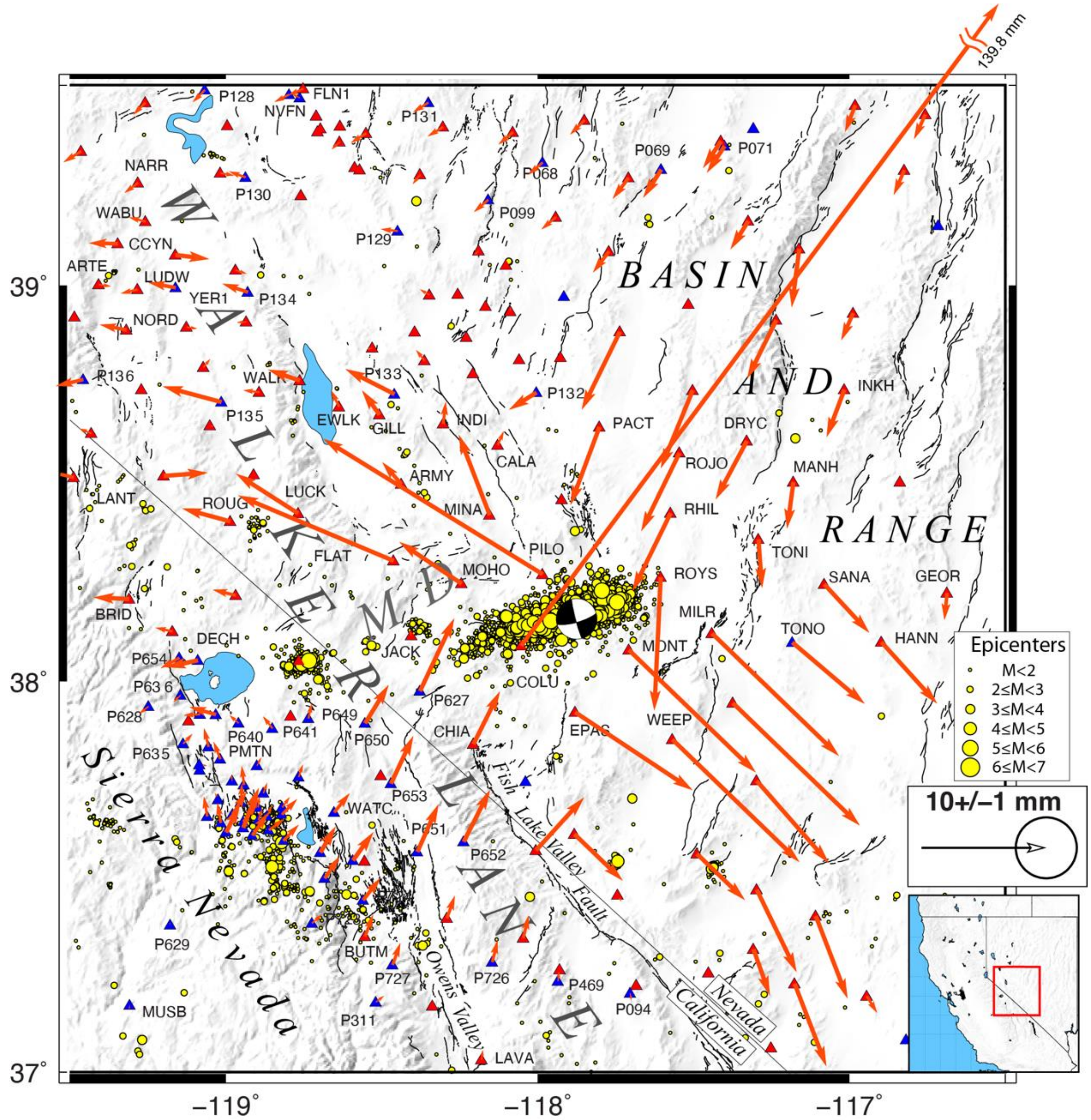

__Figure 1.__ Red vectors are coseismic displacements from May 15, 2020, M6.5 Monte Cristo Range earthquake measured with the regional GPS networks. Using this vector scale emphasizes the extent and pattern of the coseismic displacement in the medium- to far-field but makes the displacement of the station nearest to the epicenter (139.8 mm at COLU) extend beyond the figure bounds. Regional seismicity in the year 2020 is shown with yellow circles. Figure from Hammond et al., 2020 (SRL). Moment tensor and seismicity locations are from the Nevada Seismological Laboratory.

Seismic profiling across the Eglington and Frenchman Mountain faults, Las Vegas, Nevada

Lee M Liberty, Boise State University, lliberty@boisestate.edu
Seth M. Dee, Nevada Bureau of Mines and Geology, University of Nevada Reno, sdee@unr.edu

ABSTRACT

We explore the geometry and history of motion of two fault systems that extend through the Las Vegas metropolitan area. The 11-km long intrabasin Eglington fault, part of the Las Vegas Valley fault system, is expressed as a surface warp in Quaternary sediments. Hypotheses regarding the mechanisms responsible for Eglington warp formation include: coseismic warping, climatically modulated tectonic displacement, and differential sediment compaction. Results from a new 1.5 km long seismic profile reveal that the warp and associated scarps are underlain by a broad deformation zone. From 200 to 1000 m depth, reflectors are truncated, tilted, and offset, interpreted as a high-angle fault zone. The association of the surficial warp with a subsurface fault zone extending to such depths is consistent with a tectonic origin. The upper 200 m of the profile images tilted and offset reflectors with dips and displacements that are discordant from the underlying reflections. A reflection image with a hand-pulled seismic streamer, with a focus on the upper 10's of meters, is consistent with deformation extending into the shallowest sediments. The discordant, near-surface deformation is at the stratigraphic levels most influenced by late Pleistocene climatically driven ground-water level changes. These results suggest that both tectonic and non-tectonic processes may contribute to deformation along the Eglington fault.

The Frenchman Mountain fault system is a 33-km long, arcuate (convex-west), west-dipping, range-bounding normal and dextral-oblique fault on the eastern side of the Las Vegas metropolitan area. The main Quaternary trace of the northern section of the fault system is expressed as a zone of scarps in alluvial fan surfaces. Two new seismic profiles across this fault section illustrate its subsurface geometry. The main Quaternary scarp, previously identified as a ~60-70° west-dipping fault, intersects a prominent ~30° west-dipping reflector on both profiles that we interpret as a low-angle normal fault that separates late-Cenozoic sediments from older bedrock. The high-angle fault does not measurably offset the low-angle fault at the resolution of the profiles, thus constraining total vertical displacement to less than 10s of meters. Exposed on the footwall side of the Quaternary fault scarp, is a 35° west-dipping fault that may correlate with the low-angle fault imaged in the profile, further constraining total vertical displacement across the steeply dipping fault to < 10s of meters. Imaged on the Owens Avenue profile are strata of probable Miocene age in the low-angle fault's hanging wall that are warped into a rollover anticline geometry and faulted against Precambrian basement. A prominent gravity gradient immediately west of our profiles suggest an additional high-angle fault bounds the deepest part of the Las Vegas basin and accommodated the bulk of late-Cenozoic basin formation.

RECENT DEVELOPMENTS IN SEISMIC MONITORING IN NEW MEXICO

Mairi Litherland, New Mexico Bureau of Geology and Mineral Resources, mairi.litherland@nmt.edu
Amy Record, New Mexico Bureau of Geology and Mineral Resources, amy.record@nmt.edu

ABSTRACT

New Mexico experiences a moderate level of naturally occurring seismicity, primarily along the Rio Grande Rift that runs N-S along the center of the state, along with induced seismicity in oil and gas producing basins. The New Mexico Tech Seismological Observatory (NMTSO) began recording earthquakes in New Mexico in 1960 at station SNM, 5 km west of Socorro, NM. Since then, the network has expanded over time, and at present the NMTSO operates a total of 23 stations to monitor seismic activity throughout the state, with a mix of single-component short-period and three-component broadband stations. The University of New Mexico, Los Alamos National Laboratory, the United States Geological Survey, and the state of Texas maintain additional stations in and around New Mexico. A number of additional seismic stations have been installed in just the past several years as a response to the rapid increase in induced seismicity in New Mexico, particularly in the Permian Basin in southeastern New Mexico. The NMTSO has also begun using Seiscomp for routine earthquake processing as well as incorporating machine learning methods for earthquake detection. These increased capabilities have been essential to assisting regulatory agencies with strategies to manage induced seismicity and informing the public about seismic hazard in the state. Ongoing projects are using template matching and machine learning to improve catalog completeness, and earthquake relocation methods to improve location accuracy. Future projects will examine the association between fluid injection/fracking and seismicity and expand network capabilities in parts of the state that currently lack monitoring coverage.

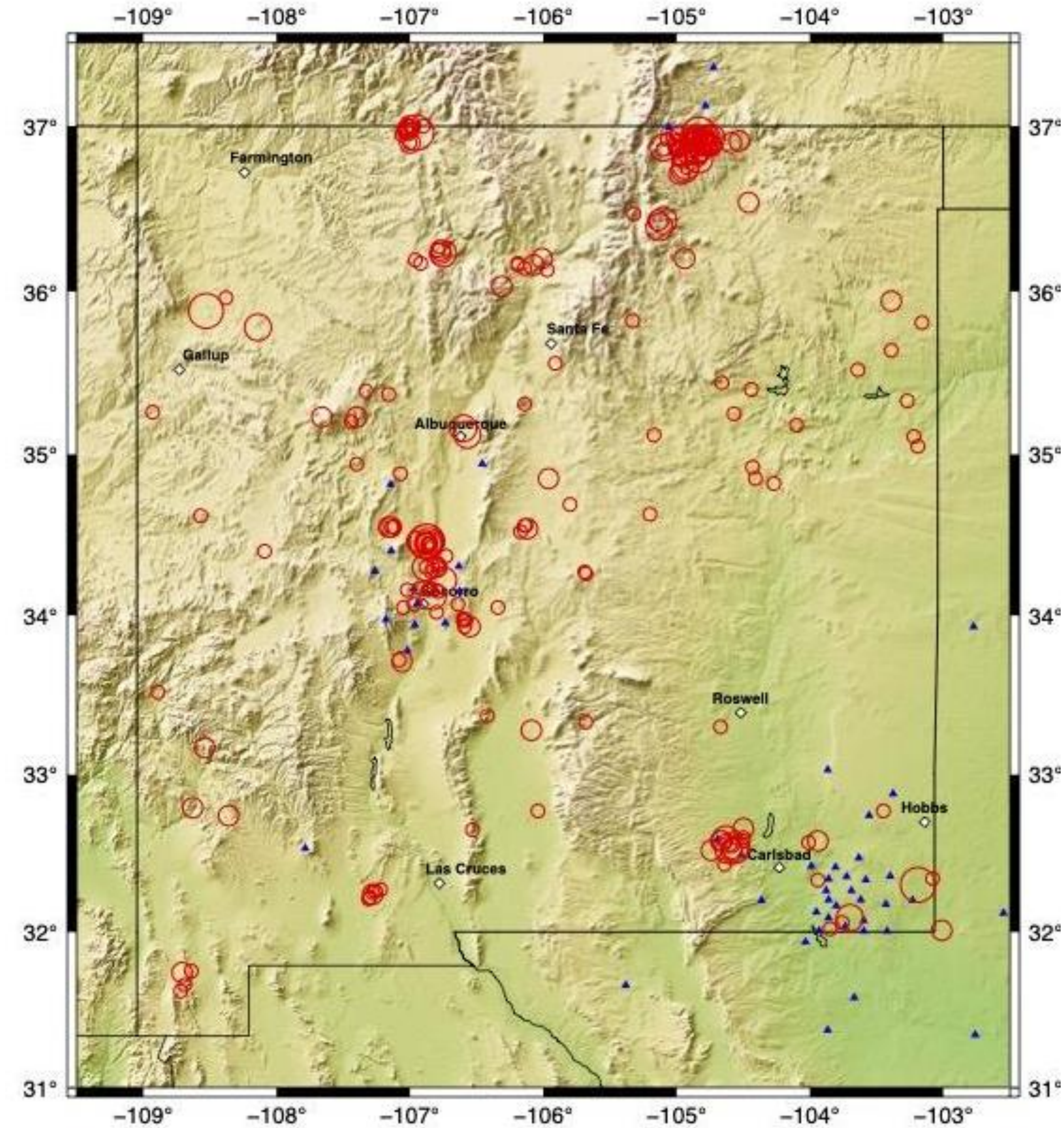

Figure 1. *Earthquakes >M3.0 from the NMTSO and USGS catalogs from 1962-2021; the magnitude of the event is represented by the size of the circle (ranging from M3 to M5). Publicly available seismic monitoring stations in New Mexico and selected stations from neighboring states are represented by blue triangles.*

EXPLORING BASIN AMPLIFICATION WITHIN THE RENO METROPOLITAN AREA WITH NON-ERGODIC 3D SCENARIOS

John N. Louie, Nevada Seismo Lab, louie@unr.edu
Lauren M. Lewright, LDEO, laurenlewright@gmail.com
Eric Eckert, Colorado State Univ., Eric.Eckert@colostate.edu
Michelle Scalise, Nevada Seismo Lab, michellescalise@nevada.unr.edu
Aditya Prathap, Univ. of Nevada, Reno, aditya.prathap.h@gmail.com
Ken Smith, Nevada Seismo Lab, ken@unr.edu

ABSTRACT

The Reno metropolitan area is subjected to significant seismic risk, primarily resulting from the region's proximity to the Mount Rose fault system and the urban area's presence within a large complex of thin (< 1 km thick) sedimentary sub-basins. Numerous paleoseismic studies have shown the Mount Rose fault system has a history of producing large Holocene earthquakes. To help explore this hazard, we used SW4, a physics-based wave-equation modeling tool, to develop a suite of non-ergodic scenarios at low frequency (<1 Hz) as well as the Reno ShakeOut Scenario at <3.1 Hz. The 3.1 Hz scenario uses a grid with a minimum spacing of 20 m with eight points per minimum wavelength to perform a full 3D simulation for a potential magnitude 6.3 earthquake within the Mount Rose fault system. This calculation is limited to a minimum shear-wave velocity (Vs min) of 500 m/s. Results at 3 Hz indicate that there is a potential for widespread and variable ground shaking at modified Mercalli intensity (MMI) between VII and VIII (very strong to severe ground shaking), with some areas achieving violent (IX and X) motions. Distributions of high shaking are controlled by proximity to the rupture, geotechnical shear-wave velocity, topography; and significantly, basin geometry. Comparisons between SW4 peak ground velocity (PGV) computations, and PGV estimates calculated from the Campbell and Bozorgnia empirical ground-motion model emphasize the degree to which very thin basins may result in greater hazard than is currently predicted. Non-ergodic scenarios for small earthquakes in and around the city suggest basin amplifications commonly exceed a factor of 4 between 0.3 and 0.8 Hz. These amplifications develop despite the thickness of low-velocity sediments below Reno rarely exceeding 1 km. This information helps improve our understanding of regional risk by highlighting these significant basin effects and the local variability that is likely to occur with any large seismic event.

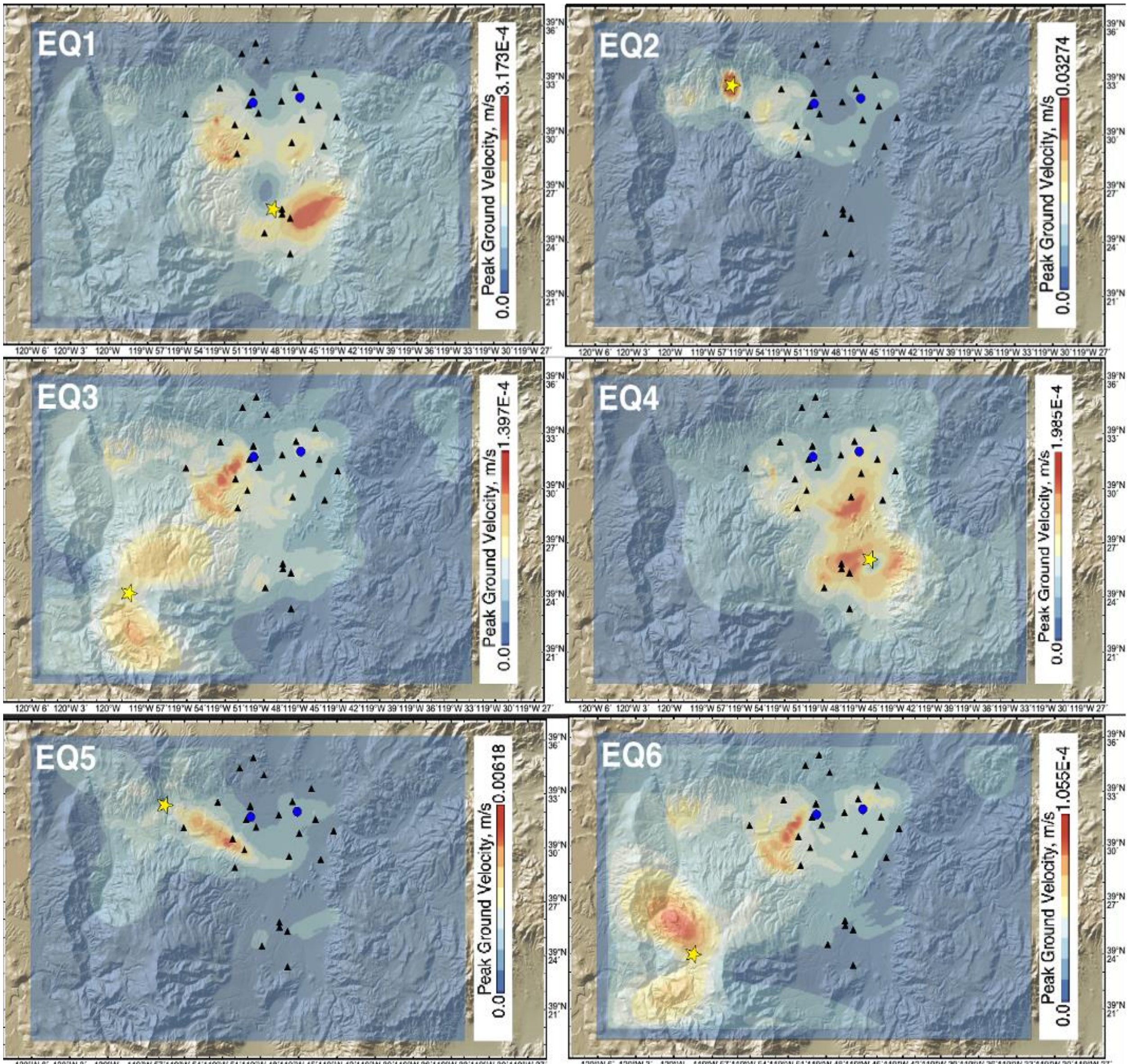

Figure 1. *Peak ground velocity (PGV) computed for frequencies up to 0.74 Hz for six M3-M4 earthquakes in the Reno area. Station locations marked by black triangles; yellow stars indicate quake epicenters. Note each quake's PGV shaking map has a different color scale. EQ2 and EQ5 were <3 km deep events in the Mogul area; the others were >6 km deep.*

MODELING AFTERSHOCK SEQUENCES IN THE EASTERN INTERMOUNTAIN WEST

Maria Mesimeri, Swiss Seismological Service, ETH, maria.mesimeri@sed.ethz.ch
Kristine L. Pankow, University of Utah Seismograph Stations, kris.pankow@utah.edu

ABSTRACT

Operational aftershock forecasting (OAF) is a relatively new product provided by the U.S. Geological Survey (USGS). It has been shown that aftershock model parameters, such as productivity and decay vary regionally. In the USGS models, the Intermountain West (IMW) is grouped into a larger area that includes much of the western U.S. In this study, we acquire earthquake catalogs from the University of Utah Seismograph Stations and the Montana Bureau of Mines and Geology (MBMG), combined with sequence specific catalogs for $M \geq 5.0$ mainshocks. Using the UUSS and MBMG catalogs, we first identify earthquake sequences ($M_{max} \leq 5.0$) that are clustered in space and time, and then sort the sequences into mainshock-aftershock sequences and earthquake swarms based on high order statistics of the moment release history (i.e. skewness and kurtosis). For each mainshock-aftershock sequence, both from the clustering analysis and the sequence specific catalogs, we model the productivity and decay properties. We find that the aftershock sequences differ from the model currently used in USGS OAF. Additionally, we report that there are differences in model parameters for different magnitude ranges, and therefore we propose three magnitude-dependent models. Interestingly, for the largest magnitude range, $M > 6$, the productivity is much less than what is found for the smaller magnitude events. Furthermore, we find that many of the earthquake sequences identified in the UUSS and MBMG catalogs are earthquake swarms. In Utah, the swarms are more geographically isolated, but in Montana occur more regionally. This result underscores the necessity of OAF for earthquake swarms, especially for regions where earthquake swarms are frequent, like the eastern IMW.

A LOGIC TREE FOR THE SUBSURFACE GEOMETRY OF THE SALT LAKE CITY SEGMENT OF THE WASATCH FAULT IN LIGHT OF THE 2020 MAGNA, UTAH EARTHQUAKE

James C. Pechmann, University of Utah, james.pechmann@utah.edu
Ivan G. Wong, Lettis Consultants International, wong@lettisci.com
Christopher B. DuRoss, U.S. Geological Survey, cduross@usgs.gov
Michael D. Hylland, Utah Geological Survey, mikehylland@utah.gov
Anthony J. Crone, U.S. Geological Survey (retired), ajcrone65@gmail.com
Stephen F. Personius, U.S. Geological Survey (retired), greenmtn1@yahoo.com
Adam P. McKean, Utah Geological Survey, adammckean@utah.gov
Walter J. Arabasz, University of Utah, wjax99@gmail.com
David P. Schwartz, U.S. Geological Survey, dschwartz@usgs.gov
Susan S. Olig, Olig Seismic Geology, oligseismicgeo@gmail.com
William R. Lund, Utah Geological Survey, williamlundugs@gmail.com
David A. Dinter, University of Utah, david.dinter@utah.edu

ABSTRACT

The 2020 M_w 5.7 Magna earthquake was the largest, and most damaging, earthquake to occur in Utah since the 1992 M_w 5.5 St. George earthquake. Long-period regional waveform modeling, in combination with the aftershock distribution, indicates that the Magna mainshock occurred 10.5 ± 2 km below the northwestern Salt Lake Valley on an oblique-normal fault dipping 34°-39° W (Fig. 1a). Published studies have interpreted the mainshock rupture to be on the Salt Lake City segment of the Wasatch fault (SLCS), which dips 70° WSW along the nearest surface trace 15 km ENE of the epicenter. This interpretation implies a listric geometry for the fault, i.e., a dip that decreases downward. The existence of the E-dipping West Valley fault zone (WVFZ), located 3-10 km W of the northern half of the SLCS, provides independent evidence of a listric geometry for this part of the SLCS. A decrease in dip on the SLCS below where it intersects the WVFZ would permit both of these faults to slip without offsetting each other, forming a large-scale backtilt graben system. The estimated ratio between the vertical slip rates on the WVFZ and the SLCS is 0.09-0.42, which provides a weak model-dependent constraint on the dip change of the SLCS. Nevertheless, even if a listric model for the northern SLCS is assumed, the precise subsurface fault geometry remains uncertain. We also cannot rule out the possibility that the Magna earthquake occurred on a W-dipping subsidiary fault in the hanging wall of the SLCS.

Here we present a logic tree of four possible models for the subsurface geometry of the SLCS that are consistent with data from the Magna earthquake and the WVFZ. In all four models the southern half of the SLCS (the Cottonwood section) has a planar geometry with an asymmetric weighted W dip distribution of 35°(0.3)–50°(0.5)– 65°(0.2). This planar model is like models formerly used for the entire Wasatch fault, but with slightly more weight on the lower-angle dips. For the northern half of the SLCS (the Warm Springs and East Bench sections) the four models (with weights) are: (1) Planar, with the same dip distribution as the Cottonwood section (0.2); (2) Listric, with the possible added complication of a “ramp-flat” geometry around

the mainshock rupture (0.4, Fig. 1b); (3) Minimally listric (0.2, Fig. 1c); and (4) Deep listric (0.2, Fig. 1d). The Magna earthquake is on or near the SLCS in the 35°-dipping branch of Model 1 and in Models 2 and 3, which have a combined weight of 0.66; in Model 4 and in the other branches of Model 1, this earthquake is on a subsidiary fault in the SLCS hanging wall. The new logic tree incorporates a plausible range of uncertainties in the subsurface geometry of the SLCS. Using this logic tree for probabilistic seismic hazard analyses, instead of the previously-favored planar models with dips of 50° ± 15°, will increase the predicted ground shaking hazard in the NW Salt Lake Valley because of the shorter average distances to the SLCS.

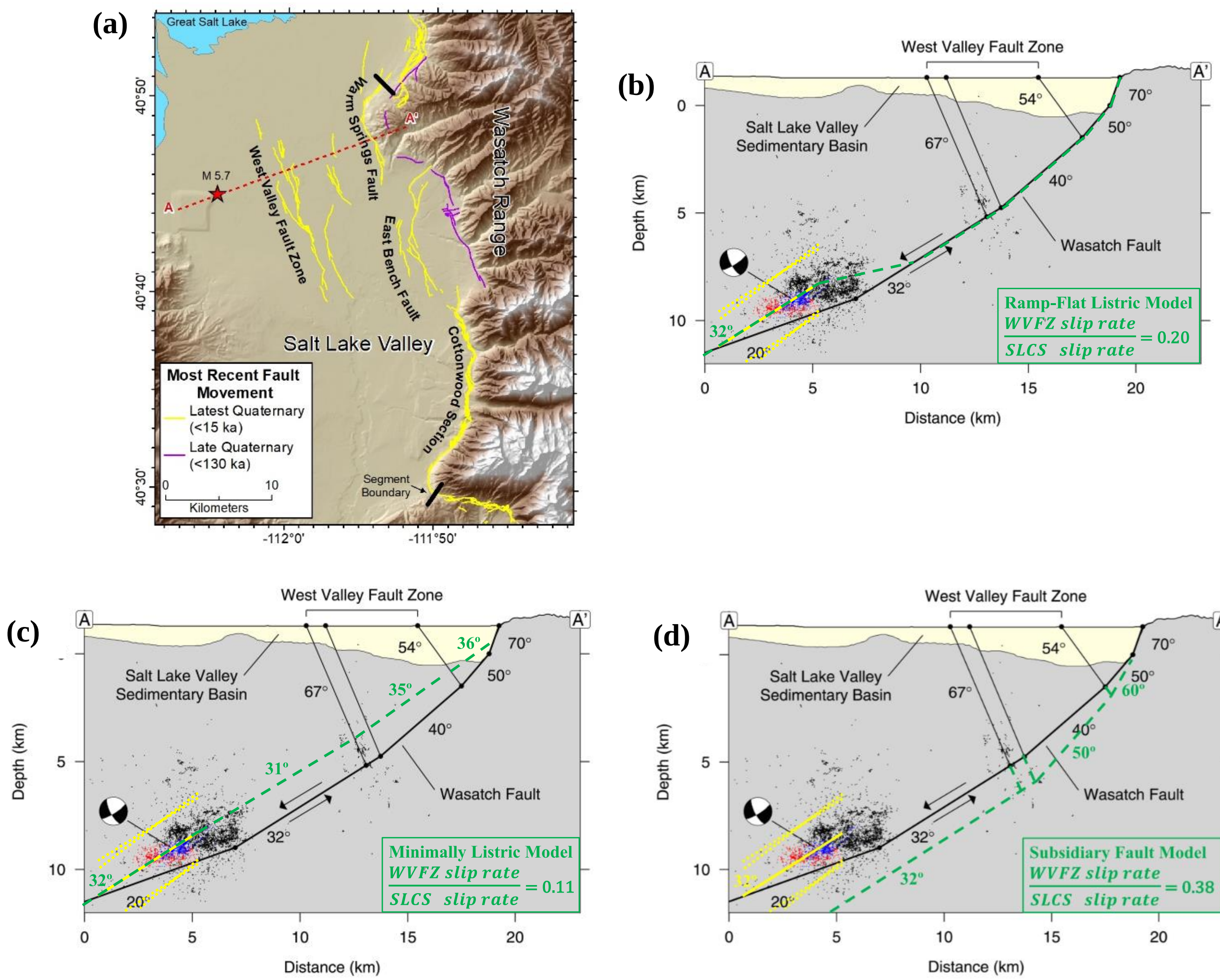

__Figure 1.__ (a) Map showing late Quaternary fault traces from the Utah Geological Survey, the epicenter of the M_w 5.7 Magna earthquake (red star), and the line of the cross sections in the other panels. (b)-(d) Hypocentral cross sections of the Magna sequence from March 18 through April 30, 2020, modified from Fig. 3 of Pang et al. (2020, GRL, e2020GL089798). The solid black lines show Pang et al.'s interpretation of the subsurface fault geometry. The dashed green lines show alternative subsurface geometries for the Wasatch fault (Models 2-4). The green box in each panel shows the predicted slip rate ratio between the West Valley fault zone and the Salt Lake City segment for the dashed green fault model. The dotted yellow lines are projections of the W-dipping nodal planes from four mainshock moment tensor solutions. Each projection passes through the centroid depth at the mainshock epicenter and extends ~1.5 km updip and ~4 km downdip from there, consistent with source studies. The solid yellow line is the projection of the W-dipping nodal plane of the University of Utah solution, shifted to 9 km depth at the epicenter.

Four decades of seismic swarm activity in the transition zone between Basin-and-Range and Colorado Plateau, Central Utah

Gesa M. Petersen, University of Utah Seismograph Stations, gpetersen@seis.utah.edu
Katherine Whidden, University of Utah Seismograph Stations, katherine.whidden@utah.edu
Kristine L. Pankow, University of Utah Seismograph Stations, Kris.Pankow@utah.edu

ABSTRACT

Central Utah is situated in the transition zone between the Basin and Range province and the Colorado Plateau. The complex geotectonic setting is not only shaped by horst and graben structures related to the E-W extension, but also by transecting E-W striking transverse structures, Mesozoic thrust fault systems, Cenozoic to Quaternary volcanism, hot springs, and increased heat flow. Seismic activity is mostly of low to moderate magnitudes, but includes a number of historical large and destructive events.

Seismically, central Utah is considered part of the Intermountain Seismic Belt, spanning from S Nevada/ N Arizona to NW Montana with dominant normal faulting and additional strike-slip faulting mechanisms. Seismic swarms in central Utah have been observed by different authors in the past and attributed to either normal faults that are associated with the divides between basin and ranges and/or to fluid migration. Over the last four decades, the seismic station coverage in the area increased significantly, resulting in decreased detection thresholds and increased location accuracy. Here we revisit the entire digital seismic catalog of the University of Utah Seismograph Stations (1981-2022) and perform a statistical analysis of seismic sequences within the catalog. We evaluate typical features of swarms in the area and interpret them in relation to newly derived focal mechanisms and geotectonic background information.

Furthermore, we perform in-depth analyses of four interesting seismic sequences, namely the 2011 Circleville seismic sequence, a seismic swarm in the Mineral Mountains in 2020, a massive seismic swarm close to Milford, 2021, and a small seismic swarm in the Sevier Valley in February 2022. By using advanced techniques for event detections, relocations, full waveform-based moment tensor inversions, and waveform similarity-based clustering, we obtain new insights into the process of the swarms and the geometry of activated faults. We infer and discuss possible triggering mechanisms and attempt to integrate our findings into the larger seismo-geo-tectonic context of the transition zone.

STRUCTURAL IMMATURITY AND TECTONIC IMPLICATIONS OF THE 2020 M_w 6.5 MONTE CRISTO RANGE EARTHQUAKE, NEVADA: EVIDENCE FROM NEAR-FIELD AND FAR-FIELD OBSERVATIONS

Israporn Sethanant, University of Victoria, isethanant@uvic.ca
Edwin Nissen, University of Victoria, enissen@uvic.ca
Léa Pousse-Beltran, University of Victoria, pousselea@gmail.com
Eric Bergman, Global Seismological Services, bergman@seismo.com
Harley M. Benz, United States Geological Survey, benz@usgs.gov
Ian Pierce, University of Oxford, ian.pierce@earth.ox.ac.uk

ABSTRACT

The 2020 M_w 6.5 Monte Cristo Range earthquake (MCRE) is the largest instrumental event in the Mina deflection zone, a pronounced E-trending jog linking NW-striking faults within the Walker Lane. The MCRE mostly ruptured previously unmapped faults, motivating us to characterize the earthquake behavior along structurally-immature faults within a highly-distributed faulting region. We use Sentinel-1B Interferometric Synthetic Aperture Radar (InSAR) data and regional GNSS coseismic offsets from the Nevada Geodetic Laboratory to model the causative faulting and slip distribution of the MCRE. Modeling results show that three faults yield the lowest misfit between data and model interferograms visually and quantitatively. The central and eastern faults strike ENE and have dominant left-lateral motions; however, the western fault strikes NE and exhibits a large extensional component (rake -47°). Maximum slip of 1.1 m occurs on the central fault plane at 8–10 km depth, but less than 0.2 m of slip reaches the surface, indicating a pronounced shallow slip deficit of 86%. We also relocate 197 hypocenters of the MCRE sequence using *mloc* software. The calibrated relocation indicates that the mainshock initiated at 9 km depth and aftershock focal depths range from 1 to 11 km, helping constrain the local seismogenic thickness and the bottom depth of our slip model. Most aftershocks are located south of the surface projection of the model faults, supporting the southward dip inferred from InSAR modeling. In addition, we calculate the regional moment tensor solutions for the 90 best-recorded events. The aftershocks exhibit a wide variety of normal and strike-slip mechanisms and orientations, and several non-double couple mechanisms. We further present new coseismic fracture observations made from drone surveys and field data, shedding light on the complex kinematics of the western rupture zone. The systems of cracks exhibit 'pebble-clearing' patterns mainly on the southeast side of each crack, implying down-to-the-northwest block motion and revealing a paired fault system below the InSAR model spatial resolution. The segmented fault geometry, pronounced shallow slip deficit, the distributed fractures, off-fault aftershocks and their various focal mechanisms, and the limited expression of long-term tectono-geomorphic features suggest that the MCRE ruptured along a structurally complex and immature fault system. This may reflect that the Mina deflection faults, which are thought to rotate clockwise about vertical axes, are diverted away from being favorable to slip, preventing the emergence of a single through-going fault that could attain structural maturity.

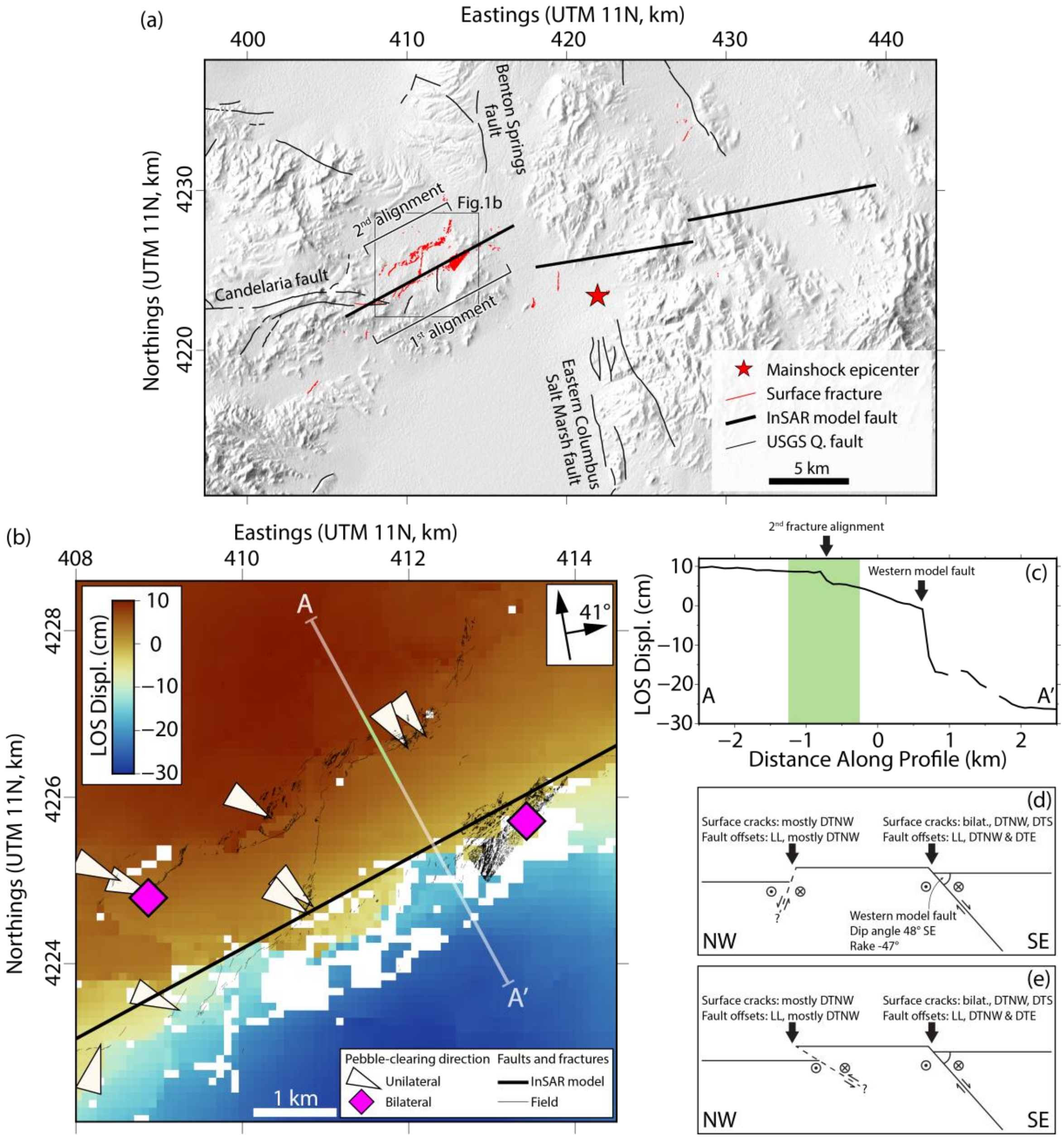

Figure 1. *(a) Hillshade map showing our relocated MCRE mainshock epicenter (red star), MCRE surface faulting and cracks mapped in the field (Dee et al., 2021; Koehler et al., 2021) (thin red lines), surface projections of our InSAR-GNSS model faults (thick black lines), and active faults from the USGS Quaternary fault and fold database (thin black lines). The inset box indicates the extent of panel (b). (b) Unwrapped ascending interferogram of the western MCRE rupture area showing the line-of-sight (LOS) displacement jump along the surface projection of the western model fault (thick black line). Thin black lines indicate fault offsets and cracks mapped in the field. The white triangles and magenta diamonds represent the location of fracture sets that exhibit unilateral and bilateral pebble clearings, respectively. Triangle tips point to the cleared pebble side or upthrown direction of the fracture. (c) Transect of unwrapped LOS displacements along A–A' in panel (b). The shaded area illustrates a secondary LOS displacement discontinuity which co-locates with the second fracture alignment. (d,e) Two, competing, interpreted cross-sections of the fault structure and kinematics in the western MCRE, derived from combining near- and far-field observations. The SE-dipping solid black line is the InSAR western model fault. Dashed black lines are the interpreted (d) NW-dipping normal- sinistral and (e) SE-dipping reverse-sinistral oblique faults beneath the second fracture sets with DTNW sense of throw. Abbreviations: bilat—bilateral; DTE—down-to-the-east; DTNW—down- to-the-northwest; DTS—down-to-the-south; LL—left-lateral. Abbreviated References: Dee et al., 2021, Technical Report 190, University of Nevada, Reno, Nevada; Koehler et al., 2021, SRL 92(2A), 823–839.*

RELOCATING THE UTAH MAGNA AFTERSHOCK SEQUENCE USING NonLinLoc, SOURCE-SPECIFIC STATION TERMS, AND WAVEFORM SIMILARITY

Daniel Wells, University of Utah, u0770911@utah.edu, danedwells@gmail.com
Anthony Lomax, Alomax Scientific, anthony@alomax.net
Benjamin Baker, University of Utah, ben.baker@utah.edu
Kristine Pankow, University of Utah, kris.pankow@utah.edu

ABSTRACT

On March 18, 2020, a magnitude 5.7 earthquake hit the Salt Lake Valley. This mainshock triggered a series of approximately 2600 aftershocks over the ensuing months, a small but significant number of which were felt by the local population. Using a dense geophone deployment and machine learning, an additional several thousand events were detected and located. Currently, both the mainshock and the majority of the aftershocks are suspected to have occurred on or near a deeper portion of the Wasatch Fault. However, a small subset of aftershocks may have occurred on a portion of the more steeply dipping and poorly understood West Valley Fault system, which is likely subsidiary to the Wasatch Fault. Unfortunately, the catalog locations and limited number of resulting focal mechanisms for this subset of aftershocks provides only a crude constraint on the true fault structure. We attempt to relocate the UUSS catalog and the machine learning catalog to better constrain the true fault structure. Preliminary relocations of the UUSS catalog using the NonLinLoc software and source specific station terms, for both 1D and 3D velocity models, suggests that the events located near the West Valley Fault system actually occurred on the Wasatch Fault. These results suggest that the Wasatch Fault is minimally listric in contrast to what has been previously proposed. Future relocations will include waveform similarity to further refine absolute locations.

THE IMPLICATIONS OF A LISTRIC WASATCH FAULT FOR SESIMIC HAZARD ALONG UTAH'S WASATCH FRONT

Ivan G. Wong, Lettis Consultants International, wong@lettisci.com
Patricia A. Thomas, Lettis Consultants International, thomas@lettisci.com
James C. Pechmann, University of Utah, james.pechmann@utah.edu

ABSTRACT

Observations of the 2020 moment magnitude (**M**) 5.7 Magna earthquake suggest that the event occurred on the Warm Springs section of the Salt Lake City segment of the Wasatch fault (Figure 1). This interpretation is still uncertain, but if correct it requires a listric geometry for this section of the fault. Whether a listric Warm Springs section is representative of the whole Salt Lake City segment, and possibly more of the Wasatch fault, has significant implications for hazard and risk along the Wasatch Front. The Wasatch fault has traditionally been modeled in seismic hazard analyses as a moderately-dipping (50° ± 15°) planar normal fault. This assumed fault geometry is embedded in both site-specific and regional seismic hazard analyses, including the USGS National Seismic Hazard Maps and hence the Utah and International Building Codes. To illustrate the impact of fault geometry on seismic hazard estimates in the Salt Lake Valley, we performed a probabilistic seismic hazard analysis (PSHA) for three representative sites (Figure 1) using both listric and planar Wasatch fault models. The models are from a logic tree developed during discussions with the Working Group on Utah Earthquake Probabilities (WGUEP) to address the epistemic uncertainties in the geometry of the Wasatch fault. This logic tree has four possible models for the Salt Lake City segment that are consistent with the available observations of the 2020 Magna earthquake and their uncertainties. The other inputs into the PSHA include a partially time-dependent Wasatch Front seismic source model based on the WGUEP model and the NGA-West2 ground motion models. We use an average site condition typical of the Quaternary sediments in Salt Lake Valley with a Vs30 of 300 m/sec.

The PSHA results indicate that the seismic hazard for a listric Wasatch fault relative to that of a moderately-dipping planar fault increases with increasing distance from the surface trace of the Wasatch fault. On the west side of the Salt Lake Valley, the increases in probabilistic ground motions for listric models compared to planar models with 50° ± 15° dips range up to 24% for peak horizontal ground acceleration and 40% for horizontal 1.0 sec spectral acceleration. The listric models result in higher hazard in this area because of the generally shorter distances from the fault to the ground surface, combined with enhanced hanging-wall effects. Hence, if the Warm Springs section of the Salt Lake City segment is listric, the National Seismic Hazard Maps underestimate the hazard in western and central parts of the Salt Lake Valley. If other sections of the Wasatch fault are listric, the hazard has also been underestimated along parts of the adjacent Wasatch Front. This potentially increased seismic hazard has implications for seismic design and risk.

Figure 1. *Sections of the west-dipping Salt Lake City segment of the Wasatch fault zone (Warm Springs, East Bench, and Cottonwood) and the east-dipping West Valley fault zone. The red lines show the surface traces of these active faults. Bold red arrows mark the Salt Lake City segment boundaries. The yellow squares mark our study sites at Temple Square, the Salt Lake City International Airport, and the town of Magna. (Figure modified from the Utah Geological Survey).*

INTERSEISMIC STRAIN ACCUMULATION ACROSS THE CENTRAL BASIN AND RANGE: IMPLICATIONS FOR SOUTHERN NEVADA SEISMIC HAZARD

Zachary M. Young, Nevada Geodetic Laboratory, zyoung@nevada.unr.edu
Corné Kreemer, Nevada Geodetic Laboratory, kreemer@unr.edu
William C. Hammond, Nevada Geodetic Laboratory, whammond@unr.edu
Geoffrey Blewitt, Nevada Geodetic Laboratory, gblewitt@unr.edu

ABSTRACT

Crustal deformation in the central Basin and Range between the Colorado Plateau and the Eastern California Shear Zone is active but slow, making it a challenge to assess how strain is distributed and crustal motion transferred. However, knowledge of strain rates is very important, particularly for addressing the seismic hazard for both the Las Vegas urban area and the site of the proposed Yucca Mountain nuclear waste repository, in southern Nevada. Global Positioning System (GPS) data provide important constraints, particularly now that the GPS network in the area has substantially expanded in recent years. However, because deformation is slow, it is important to mitigate any transient tectonic and non-tectonic signals to obtain the most accurate long-term interseismic motion and use robust estimation of strain rates. We use data from all GPS stations in the region, including both long-running continuous and semi-continuous stations. Postseismic displacements at these stations are modeled and removed using source parameters for 41 events, dating back to the 1700 Cascadia megathrust earthquake, and are found to contribute significantly to the deformation field within the central Basin and Range. While the postseismic field is dominated by a few large events, we find the cumulative contributions from events which are individually insignificant are large enough to alter the velocity gradients of the region. We also remove regionally correlated noise from the time series with the Common Mode Component Imaging technique. The removal of both the postseismic transients and common-mode noise substantially reduces the velocity uncertainties, by 62.1% in the east component and 53.8% in the north and improves the spatial coherency of the velocity field. We find deformation is active within the Las Vegas Valley with east–west extension 0.5 – 0.6 mm/yr. Furthermore, the interseismic strain rate field, calculated with the final velocities, reveals higher strain rates through southern Nevada than in previous studies, with rates within the Las Vegas Valley of 8.5 ± 2.4 $\times 10^{-9}$ yr^{-1}. Our results confirm shear along the Pahranagat Shear Zone but the estimated amplitude is strongly affected by postseismic relaxation.

3D SHEAR WAVE VELOCITY MODEL OF SALT LAKE VALLEY VIA SURFACE WAVES RECORDED BY THE MAGNA AFTERSHOCK NODAL ARRAY

Qicheng Zeng, University of Utah, Qicheng.Zeng@utah.edu
Fan-Chi Lin, University of Utah, FanChi.Lin@utah.edu
Amir A. Allam, University of Utah, amir.allam@utah.edu

ABSTRACT

We deployed 168 three-component nodal geophones across Salt Lake Valley between March 18 and April 30 in 2020 in response to the M5.7 Magna earthquake. On March 31, 2020, a M6.5 earthquake struck central Idaho. In this study, we aim to construct a 3D shear velocity model of Salt Lake Valley using Rayleigh waves excited by the Idaho earthquake and observed across the temporary nodal array as well as 49 stations of the regional network. We show that Rayleigh wave ellipticity or horizontal to vertical (H/V) ratios between 10 and 20 sec period can be measured using the direct Rayleigh wave. Moreover, we show that additional H/V ratios can be measured down to 5 sec period using the multi-component earthquake coda cross-correlations. Clear correlations are observed between the measured H/V ratios and known basin structure, where high H/V ratios are observed in areas associated with thick unconsolidated sediments. Taking the advantage of the outstanding shallow sensitivity of the H/V ratios, we invert for a 3D Vs model of the Salt Lake Valley with homogeneous Rayleigh wave phase velocities between 5 and 20 sec period as additional constraints for deeper structure. Our model complements the current Community Velocity Model (CVM), which is mostly constrained by borehole and gravity measurements, and opens up future opportunities to update the CVM that is critical for regional seismic assessment.